

NANOSTRUCTURES

RADIATION STABILITY OF CARBON NANOSTRUCTURES

G. Ya. Gerasimov

UDC 537.533.9

A theoretical study of the radiation stability of carbon nanostructures irradiated by an electron beam has been made. Calculations have been performed with the use of an analytical expression for the cross-section for scattering of relativistic electrons by carbon atoms, as well as of the data on the threshold energy of atomic displacement from the carbon lattice obtained by the molecular dynamics method. Stability limits of carbon nanostructures and basic parameters of the process have been found. The calculated values of the characteristic time of the process are in good agreement with the available experimental data.

Keywords: carbon nanostructures, fullerenes, carbon nanotubes, graphene, electron beam, radiation stability.

Carbon nanostructures (CNSs) such as fullerenes, carbon nanotubes (CNTs), graphene sheets, and their derivatives occupy an important place among nanomaterials due to their unique properties that offer much promise for practical use [1, 2]. At the present time the field of use of CNSs includes optical and electronic devices [3, 4], CNS-based polymers [5, 6], composite materials [7, 8], hydrogen storage systems [9], biosensors [10], ion beam focusing systems [11], etc.

Methods for obtaining fullerenes and carbon nanotubes are rather versatile. The most widely used ones are arc discharge in the atmosphere of an inert gas with the application of graphite electrodes [12], laser irradiation of a graphite surface [13], and decomposition of hydrocarbons on the surface of a metal catalyst (CVD method) [14]. Graphene represents a monolayer from carbon atoms close-packed into a hexagonal crystal structure, which can be considered as an ideal realization of a two-dimensional material [15]. Recent advances in the technology of splitting graphite specimens into single-crystal films [16] made it possible to investigate this exotic system experimentally. As measurements show, individual graphene sheets have extraordinary electron transfer properties, which permits using this material to replace modern silicon transistors in microelectronics [17].

The use of radiation technology plays an important part in the investigation and production of nanostructured systems [18]. In particular, the interaction of high-energy electron beams with CNSs leads to their modification or to the formation of new structures, which includes welding of criss-cross CNTs [19], transformation of single-layer CNTs into multilayer ones [20], polymerization of C_{60} fullerene layers [21], clustering of C_{60} fullerenes on the surface of graphene sheets [22], radiation-chemical processes with the participation of fullerenes [23], etc.

Electron-beam irradiation of a carbon nanostructure can be considered as an initiating step leading to the formation of vacancies and other defects in its lattice. The further transformation of the structure depends on both its internal structure and its position relative to the other nanoobjects. In this connection, the problem of determining the radiation stability limits of the structure arises. In the present work, this problem has been solved with the use of the analytical expression for the cross-section for scattering of relativistic electrons by carbon atoms, as well as of the data on the threshold energy of carbon atom displacement from the CNS lattice obtained by the molecular dynamics method.

Scattering of Relativistic Electrons by the Carbon Lattice. The interaction of high-energy particles with CNSs causes various radiation effects in them, such as electron excitation or ionization of individual atoms, collective electron excitation (formation of plasmons), rupture of interatomic bonds, displacement of atoms from the lattice into the surrounding space, formation of phonons leading to a heating of the lattice, etc. [24]. These effects determine the

Institute of Mechanisms, M. V. Lomonosov Moscow State University, 1 Michurinskii Ave., Moscow, 119192, Russia; email: gerasimov@imec.msu.ru. Translated from Inzhenerno-Fizicheskii Zhurnal, Vol. 83, No. 2, pp. 369–375, March–April, 2010. Original article submitted July 14, 2009.

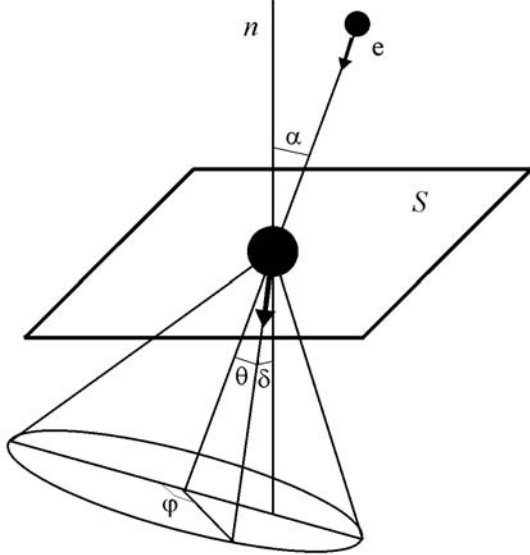


Fig. 1. Scheme of the electron-carbon-lattice-atom collision.

possible mechanisms of CNS structure collapse caused by irradiation. The most important of them are: 1) direct transfer of energy of incident particles to the intrinsic motion of lattice atoms (*knock-on* mechanism); 2) excitation of the electronic structure of the CNS followed by an excitation energy redistribution between intrinsic vibrational degrees of freedom of the macromolecule leading to its decay (*excitation* mechanism) [25]. The second mechanism, if the collapse of solid structures under the action of an electron beam is considered, is minimal in metals, semimetals, and semiconductors since the beam-initiated electron excitation is insufficiently localized for its effective transformation into kinetic energy of individual atoms of the lattice [26]. Most CNSs are metals or semiconductors [4, 27] and, therefore, it is assumed that the main mechanism of their collapse under the action of an electron beam is elastic collisions of electrons with atoms of the corresponding lattice (*knock-on* mechanism) [28].

The basic parameters determining the stability limits of the carbon lattice for a given nanostructure are electron density E , beam density j , and angle of its inclination α to the CNS surface. The typical value of the quantity E lies in the range of 100–1000 keV [24] where the motion of electrons should be considered as relativistic motion. This means that the parameter $b = v/c$ is close to unity and should be calculated by the relation $b_2 = 1 - (E/mc^2 + 1)^{-2}$. The relation between the kinetic energy of electrons E and the energy ΔE transferred to an atom of mass M in a binary collision can be written in the form

$$\Delta E = \Delta E_{\max} \cos^2 \theta, \quad \Delta E_{\max} = 2E(E + 2mc^2)/Mc^2, \quad (1)$$

where θ is the angle between the initial direction of electron motion and the direction of carbon atom displacement (see Fig. 1).

One of the main physical characteristics in investigating the radiation damage of crystals is the threshold atomic displacement energy E_d [29]. In simplified form, it is defined as the minimal energy needed for such atomic displacement from a lattice site at which a Frenkel pair is formed without its spontaneous recombination. The minimum energy of electrons E_{\min} at which displacement of carbon atoms from the lattice surface occurs is determined from (1) by replacing ΔE by E_d at $\theta = 0$. In the general case, E_d depends on the angle δ between the direction of atomic displacement and the normal to the CNS surface [30, 31].

The interaction of CNS atoms with relativistic electrons occurs in a time of the order of 10^{-21} sec and can be considered as elastic scattering of an electron by the atomic nucleus [24, 32]. The atomic displacement cross-section determining the probability of vacancy formation in the lattice can be determined on the basis of the analytical approximation [33] of the known Mott formula for the Coulomb scattering of relativistic electrons by the atomic nucleus. In the laboratory reference system, this quantity is written as

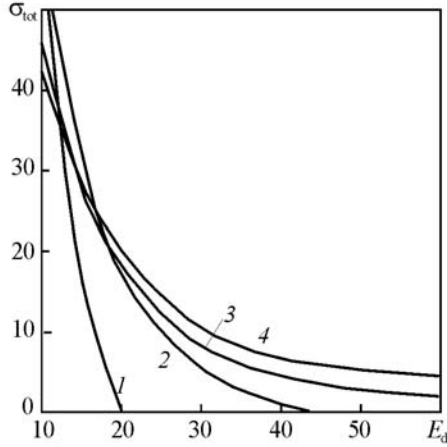


Fig. 2. Cross-section of isotropic displacement of an atom from the carbon lattice as a function of the threshold displacement energy: 1) $E = 100$ keV; 2) 200; 3) 400; 4) 800. σ_{tot} , b; E_d , eV.

$$d\sigma = r_e^2 Z^2 (1 - b^2) b^{-4} R(\theta) \sin \theta \cos^{-3} \theta d\theta d\varphi, \quad R(\theta) = 1 + \pi ab \cos \theta - (b^2 + \pi ab) \cos^2 \theta. \quad (2)$$

The total displacement cross-section σ_{tot} is obtained from (2) by integrating over angles φ ($0 \leq \varphi \leq 2\pi$) and θ . In so doing, the angle θ varies from zero to the limiting value θ_{\max} which is determined from the condition

$$\cos^2 \theta_{\max} = E_d(\delta)/\Delta E_{\max}. \quad (3)$$

For the angle δ , by means of simple geometric constructions (Fig. 1) we can obtain the relation

$$\delta = \arccos (\cos \theta \cos \alpha - \sin \theta \sin \alpha \cos \varphi),$$

which at given angles α and φ yields the relation $\delta = \delta(\theta)$. In the case where the E_d value is independent of the angle δ (isotropic displacement), integration of (2) yields for the total displacement cross-section the expression

$$\sigma_{\text{tot}} = \pi r_e^2 Z^2 (1 - b^2) b^{-4} F(\Delta E_{\max}/E_d), \quad (4)$$

$$F(x) = x + 2\pi abx^{1/2} - [1 + 2\pi ab + (b^2 + \pi ab) \ln x].$$

Results and Discussion. The dependence of the isotropic displacement cross-section σ_{tot} on the threshold energy E_d calculated by formula (4) at various energies of incident electrons E is shown in Fig. 2. It is seen that the given quantity decreases with increasing E_d at all values of E . The behavior of σ_{tot} as a function of E at a fixed value of E_d is more complicated. At threshold energies $E_d \geq 20$ eV typical of the CNS lattice an increase in the cross-section with increasing E is observed.

In the general case, integration of the differential cross-section (2) should be carried out taking into account that $E_d = E_d(\delta)$. To determine this dependence, one usually uses modeling of the process of displacement of carbon atoms from the CNS lattice by the molecular dynamics method [30, 31]. Practical application of this method requires identification of the carbon lattice, which is achieved by giving an adequate interatomic interaction potential (see, e.g., [34, 35]). As a rule, these potentials are classical in nature and do not take into account quantum-mechanical effects. An alternative approximation is the inclusion of the directionality effects of covalent bonds in Hamiltonian systems (*tight-binding* method), which permits naturally taking into account of the quantum-mechanical nature of covalent bonds in the interatomic potential [36, 37].

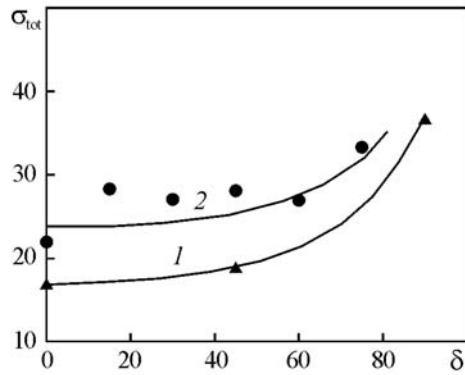


Fig. 3. Cross-section of atomic displacement from the carbon lattice as a function of the displacement angle: 1) carbon nanotube; 2) fullerene; σ_{tot} , b; δ , deg.

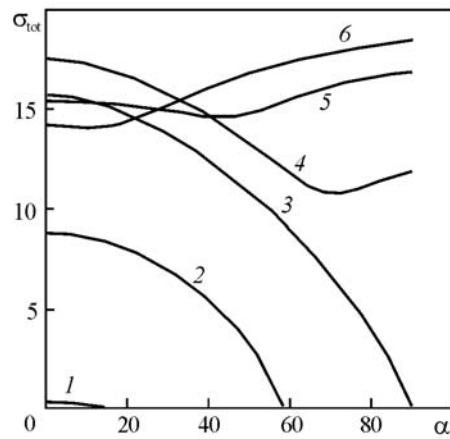


Fig. 4. Cross-section of atomic displacement from the carbon lattice as a function of the electron beam direction: 1) $E = 85$ keV; 2) 100; 3) 140; 4) 200; 5) 400; 6) 800. σ_{tot} , b; α , deg.

Modeling of the displacement of carbon atoms from the C_{60} fullerene surface was carried out in [30], where the relation $E_d = E_d(\delta)$ as applied to a spherical carbon lattice was obtained (Fig. 3). As calculations show, at transferred energies lower than E_d the considered carbon atom and its surrounding atoms experience significant deviations from their equilibrium positions and gradually go back to the state of rest. At $\Delta E > E_d$ the atom leaves the fullerene shell, with its kinetic energy on infinity even at $\Delta E = E_d$ being other than zero. Analysis of Fig. 3 shows that as the angle δ increases, there is an increase in the threshold displacement energy, which reaches its maximum at $\delta = \pi/2$. It should be noted that in virtue of the discreteness of the distribution of carbon atoms over the fullerene surface the E_d value depends also on the direction of the momentum transferred to the atom in the plane tangent to the fullerene surface.

The threshold energy E_d of carbon atom displacement from the surface of a nanotube was determined in [31] by the *tight-binding* method. As calculations show, at $\delta = \pi/2$ the displaced atom leads to a deviation from equilibrium of about ten neighboring atoms, which explains the significant value of E_d for the given displacement direction (Fig. 3). The momentum normal to the lattice surface causes minimal disturbance of the local environment of the atom being displaced. In this case, the threshold displacement energy of the atom is equal approximately to the sum of energies of its binding with neighboring atoms. The difference between the threshold displacement energies for fullerenes and nanotubes observed in Fig. 3 can be explained by the employment of different computing methods, since the geometrical features of the surface should not produce an appreciable effect on the value of the given parameter of the process [24].

The relation between the threshold displacement energy E_d and the angle δ for a carbon nanotube obtained in [31] by the molecular dynamics method has been used in the present work to calculate the displacement cross-section

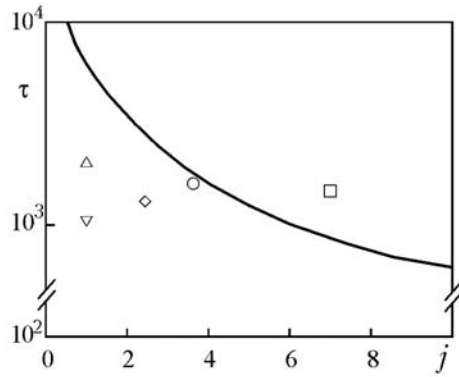


Fig. 5. Characteristic collapse time of CNSs as a function of the flow density in the electron beam. Dots show experimental data (see the text). τ , sec; j , A/cm^2 .

σ_{tot} . The dependence of the cross-section on the electron beam orientation at various energies of electrons in the beam is given in Fig. 4. Analysis of the figure shows that the nanotube begins to collapse at $E \approx 90$ keV on lattice portions normal to the beam direction. A nonzero value of the cross-section throughout the variation range of α is observed at $E \geq 140$ keV, which agrees with the experimental data of [28]. For energies of electrons in the beam higher than 200 keV the calculated cross-section σ_{tot} varies from 12 to 18 b ($1 \text{ b} = 10^{-28} \text{ m}^2$) depending on the angle of inclination of the beam to the lattice surface.

To estimate the stability of carbon nanostructures irradiated by an electron beam, we can make use of a simple relation including the basic parameters of the process. The displacement cross-section σ_{tot} divided by the area S per atom of the CNS lattice gives the probability of displacement of an atom when an electron is scattered by it. Multiplying this value by the frequency of incidence of beam electrons on a surface S equal to jS , we obtain the probability of atomic displacement in a time unit. For a given flow density, the characteristic time of the process is defined by the relation $\tau = (\sigma_{\text{tot}}j)^{-1}$. The typical value of the electron flow density in the experiment with CNSs varies over the range $1\text{--}10 \text{ A}/\text{cm}^2$ [20, 38, 39]. Figure 5 shows the dependence $\tau = \tau(j)$ at an average value of $\sigma_{\text{tot}} = 15 \text{ b}$ and its comparison with the existing experimental data on the radiation stability of carbon nanotubes and graphene sheets [10, 28, 38–40].

The triangle in Fig. 5 corresponds to experiments on the transformation of the surface of single-layer CNTs irradiated by electrons with $E = 200$ keV and $j = 1 \text{ A}/\text{cm}^2$ in a transmission electron microscope (TEM) [40]. As observations show, in a time of the order of $2 \cdot 10^3$ sec the diameter of nanotubes decreases from its initial value of 1.4 to 0.4 nm. In so doing, the cylindrical form of the tubes remains unaltered. Further irradiation causes a collapse of individual tubes. It may be suggested that the limiting case of tube modification is the formation of linear chains of carbon atoms. Analogous results for single-layer CNTs were obtained in a TEM with $E = 200$ keV and $j = 3.7 \text{ A}/\text{cm}^2$ [28] (circle in Fig. 5), where the microstructure of nanotubes after $1.56 \cdot 10^3$ sec of irradiation collapses and becomes amorphous.

The combined effect of the action of an electron beam ($E = 100$ keV, $j = 1 \text{ A}/\text{cm}^2$) and high-temperature heating (the maximal temperature of the carbon lattice is about 1200 K) on the formation of defects in CNTs was considered in [38]. The process dynamics is described by an exponential decrease in the tube diameter with a characteristic time $\tau = 10^3$ sec (inverted triangle in Fig. 5). Estimation of the threshold displacement energy E_d under the considered conditions yields a value of 5.5 eV, which is much lower than the corresponding value at room temperature. The value of the cross-section σ_{tot} in the case of isotropic displacement is equal to about 160 b (see Fig. 2). This explains the excess of the calculated value of the characteristic time of the process over the experimental one by an order of magnitude.

The characteristic time of structural transformation of a bank of fluorinated single-layer CNTs under the action of an electron beam in a TEM ($E = 300$ keV, $j = 2.46 \text{ A}/\text{cm}^2$) [20] is shown in Fig. 5 by a rhomb. The transformation process of nanotubes proceeds towards partial collapse of the bank and the formation of a structure resembling a multilayer CNT. The presence of added fluorine atoms leads to an increase in the length of the C–C bond in the tube to 0.153 nm characteristic of the diamond lattice. A decrease in the bond energy leads to a decrease in the E_d value

and, accordingly, to an increase in the cross-section σ_{tot} , which in turn decreases the characteristic time of transformation of the bank of fluorinated CNTs compared to convectional ones (see Fig. 5). A similar effect is observed in the case of electron irradiation of ozonized carbon nanotubes [41].

The defect formation dynamics in a graphene membrane irradiated by an electron beam ($E = 100$ keV, $j = 7$ A/cm²) was investigated in [39]. The corresponding process time is represented in Fig. 5 by a square. The excess of the experimental data over the calculated ones can be explained by the lower average value of the displacement cross-section σ_{tot} at $E = 100$ keV (see Fig. 4) than that used in the calculation. It should be noted that graphene membranes are fairly resistant to electrons with energy $E = 100$ keV. At least the formation of vacancies observed in [39] does not mean complete destruction of the membrane.

CONCLUSIONS

1. A brief survey of the state of the art of investigations on the application of the radiation technology for transforming carbon nanostructures shows that this scientific trend plays an important role because of the unique electronic, mechanical, and chemical properties of the materials formed, which makes them possible candidates for wide practical use in various fields: from molecular electronics to composite materials.

2. The theoretical consideration of the radiation stability of carbon nanostructures under the action of an electron beam on them has made it possible to elucidate the stability limits and the basic parameters of the process. The calculated values of the characteristic time of the process agree with the available experimental data.

This work is a part of the IAEA Program "Supporting Radiation Synthesis and the Characterization of Nanomaterials for Health Care, Environmental Protection, and Clean Energy Applications" (IAEA Regional TC Project No. RER/8/014).

NOTATION

$a = Z/137$; $b = v/c$; $c = 2.998 \cdot 10^8$ m/sec, velocity of light in free space; E , kinetic energy of electrons in the beam, eV; ΔE , energy transferred to an atom upon collision with an electron, eV; E_d , threshold energy of atomic displacement from the lattice, eV; j , electron flow density in the beam, A/m²; $m = 9.108 \cdot 10^{-31}$ kg, rest mass of an electron; M , atomic mass, kg; n , local normal to the CNS surface; $r_e = 2.818 \cdot 10^{-15}$ m, electron classical radius; R , ratio of the cross-section of electron scattering by the atomic nucleus to the Rutherford cross-section; S , area per atom of the CNS lattice, m²; v , velocity of electrons in the beam, m/sec; $x = \Delta E_{\text{max}}/E_d$; Z , atomic nucleus charge (atomic number of the element); α , angle between the beam direction and the local normal to the CNS surface; δ , angle between the direction of atomic displacement and the local normal to the CNS surface; θ , angle between the beam direction and the atomic displacement direction; σ , atomic displacement cross-section, m²; σ_{tot} , total cross-section of atomic displacement, b ($1\text{b} = 10^{-28}$ m²); τ , characteristic time of the process, sec; φ , azimuth angle in the plane normal to the beam direction. Subscripts: d, displacement; e, electron; max, maximum value; min, minimum value; tot, total.

REFERENCES

1. I. P. Suzdalev, *Nanotechnology: Physics and Chemistry of Nanoclusters, Nanostructures, and Nanomaterials* [in Russian], KomKniga, Moscow (2006).
2. B. Brushan (Ed.), *Springer Handbook of Nanotechnology*, Springer, Berlin (2007).
3. M. P. Anantram and F. Leonard, Physics of carbon nanotube electronic devices, *Rep. Prog. Phys.*, **69**, No. 3, 507–561 (2006).
4. Y.-W. Son, M. L. Cohen, and S. G. Louie, Half-metallic graphene nanoribbons, *Nature*, **444**, No. 7117, 347–349 (2006).
5. C. Wang, Z.-X. Guo, S. Fu, W. Wu, and D. Zhu, Polymers containing fullerene or carbon nanotube structures, *Prog. Polym. Sci.*, **29**, No. 11, 1079–1141 (2004).
6. S. V. Ahir, Y. Y. Huang, and E. M. Terentjev, Polymers with aligned carbon nanotubes: active composite materials, *Polymer*, **49**, No. 18, 3841–3854 (2007).

7. Y. Hu, O. A. Shenderova, Z. Hu, C. W. Padgett, and D. W. Brenner, Carbon nanostructures for advanced composites, *Rep. Prog. Phys.*, **69**, No. 6, 1847–1895 (2006).
8. T. Ramanathan, A. A. Abdala, S. Stankovich, et al., Functionalized graphene sheets for polymer nanocomposites, *Nature Nanotech.*, **3**, No. 6, 327–331 (2008).
9. M. Hirscher and M. Becher, Hydrogen storage in carbon nanotubes, *J. Nanosci. Nanotech.*, **3**, No. 1, 3–17 (2003).
10. M. Shim, N. W. S. Kam, Y. Chen, et al., Functionalization of carbon nanotubes for biocompatibility and biomolecular recognition, *Nanoletters*, **2**, No. 4, 285–288 (2002).
11. V. M. Biryukov, S. Bellucci, and V. Guidi, Channeling technique to make nanoscale ion beams, *Nucl. Instr. Meth.*, **B231**, Nos. 1–4, 70–75 (2005).
12. N. I. Alekseyev and G. A. Dyuzhev, Fullerene formation in an arc discharge, *Carbon*, **41**, No. 7, 1343–1348 (2003).
13. D. Kasuya, F. Kokai, K. Takahashi, M. Yudasaka, and S. Iijima, Formation of C₆₀ using CO₂ laser vaporization of graphite at room temperature, *Chem. Phys. Lett.*, **337**, Nos. 1–3, 25–30 (2001).
14. S. Musso, S. Porro, M. Rovere, M. Giorcelli, and A. Tagliaferro, Fluid dynamic analysis of gas flow in a thermal-CVD system designed for growth of carbon nanotubes, *J. Cryst. Growth*, **310**, No. 2, 477–483 (2007).
15. M. I. Katsnelson, Graphene: carbon in two dimensions, *Mater. Today*, **10**, Nos. 1–2, 20–27 (2007).
16. K. S. Novoselov, A. K. Geim, S. V. Morozov, et al., Electric field effect in atomically thin carbon films, *Science*, **306** No. 5696, 666–669 (2004).
17. R. Van Noorden, Moving towards a graphene world, *Nature*, **442**, No. 7100, 228–229 (2006).
18. A. G. Chmielewski, D. K. Chmielewska, J. Michalik, and M. H. Sampa, Prospects and challenges in application of gamma, electron and ion beams in processing of nanomaterials, *Nucl. Instrum. Meth.*, **B265**, No. 1, 339–346 (2007).
19. A. V. Krasheninnikiv and K. Nordlund, Irradiation effects in carbon nanotubes, *Nucl. Instrum. Meth.*, **B216**, No. 1, 335–366 (2004).
20. K. H. An, K. A. Park, J. G. Heo, et al., Structural transformation of fluorinated carbon nanotubes induced by *in situ* electron-beam irradiation, *J. Am. Chem. Soc.*, **125**, No. 10, 3057–3061 (2003).
21. J. Onoe, T. Nakayama, M. Aono, and T. Hara, The electron transport properties of photo- and electron-beam-irradiated C₆₀ films, *J. Phys. Chem. Solids*, **65**, Nos. 2–3, 343–348 (2004).
22. A. Hashimoto, H. Terasaki, A. Yamamoto, and S. Tanaka, Electron beam irradiation effect for solid C₆₀ epitaxy on graphene, *Diamond Relat. Mater.*, **18**, Nos. 2–3, 388–391 (2009).
23. D. M. Guldi, Radiation chemistry of fullerenes, *Stud. Phys. Theor. Chem.*, **87**, No. 1, 253–286 (2001).
24. F. Banhart, Irradiation effects in carbon nanostructures, *Rep. Prog. Phys.*, **62**, No. 8, 1181–1221 (1999).
25. M. R. C. Hunt, J. Schmidt, and R. E. Palmer, Electron-beam-induced fragmentation in ultrathin C₆₀ films on Si (100)-2 × 1-H: Mechanisms of cage destruction, *Phys. Rev.*, **B60**, No. 8, 5927–5937 (1999).
26. G. S. Was and T. R. Allen, Radiation damage from different particle types, in: (K. E. Sickafus, E. A. Kotomin, and B. P. Uberuaga Eds.), *Radiation Effects in Solids*, Springer, Dordrecht (2007), pp. 65–98.
27. L.-C. Qin, Electron diffraction from carbon nanotubes, *Rep. Prog. Phys.*, **69**, No. 10, 2761–2821 (2006).
28. B. W. Smith and D. E. Luzzi, Electron irradiation effects in single wall carbon nanotubes, *J. Appl. Phys.*, **90**, No. 7, 3509–3515 (2001).
29. M. Hohenstein, A. Seeger, and W. Sigle, The anisotropy and temperature dependence of the threshold for radiation damage in gold—comparison with other FCC metals, *J. Nucl. Mater.*, **169**, No. 1, 33–46 (1989).
30. F. Z. Cui, H. D. Li, and X. Y. Huang, Atomistic simulation of radiation damage to C₆₀, *Phys. Rev.*, **B49**, No. 14, 9962–9965 (1994).
31. V. H. Crespi, N. G. Chopra, M. L. Cohen, A. Zettl, and S. G. Louie, Anisotropic electron-beam damage and the collapse of carbon nanotubes, *Phys. Rev.*, **B54**, No. 8, 5927–5931 (1996).
32. M. V. Makarets, Yu. I. Prylutskyy, O. V. Ogloblya, L. Carta-Abelmann, and P. Scharff, Computer simulation of supported C₆₀ fullerenes fragmentation by particle beam, *Carbon*, **42**, Nos. 5–6, 987–990 (2004).
33. W. A. McKinley, Jr. and H. Feshbach, The Coulomb scattering of relativistic electrons by nuclei, *Phys. Rev.*, **74**, No. 12, 1759–1763 (1948).

34. J. Tersoff, Empirical interatomic potential for carbon, with application to amorphous carbon, *Phys. Rev. Lett.*, **61**, No. 25, 2879–2882 (1988).
35. D. W. Brenner, O. Shenderova, J. A. Harrison, S. J. Stuart, B. Ni, and S. B. Sinnott, A second-generation reactive empirical bond order (REBO) potential energy expression for hydrocarbons, *J. Phys.: Condens. Matter.*, **14**, No. 4, 783–803 (2002).
36. C. H. Xu, C. Z. Wang, C. T. Chan, and K. M. Ho, A transferable tight-binding potential for carbon, *J. Phys.: Condens. Matter.*, **4**, No. 28, 6047–6054 (1992).
37. S. Goedecker and L. Colombo, Efficient linear scaling algorithm for tight-binding molecular dynamics, *Phys. Rev. Lett.*, **73**, No. 1, 122–125 (1994).
38. T. D. Yuzvinsky, W. Mickelson, S. Aloni, G. E. Begtrup, A. Kis, and A. Zettl, Shrinking a carbon nanotube, *Nano Lett.*, **6**, No. 12, 2718–2722 (2006).
39. J. C. Meyer, C. O. Girit, M. F. Crommie, and A. Zettl, Imaging and dynamics of light atoms and molecules on graphene, *Nature*, **454**, No. 7202, 319–322 (2008).
40. P. M. Ajayan, V. Ravikumar, and J.-C. Charlier, Surface reconstructions and dimensional changes in single-walled carbon nanotubes, *Phys. Rev. Lett.*, **81**, No. 7, 1437–1440 (1998).
41. U. Rauwald, J. Shaver, D. A. Klosterman, et al., Electron-induced cutting of single-walled carbon nanotubes, *Carbon*, **47**, No. 1, 178–185 (2009).